Separation and Purification Technology 277 (2021) 119320

Contents lists available at ScienceDirect

Separation and Purification Technology

journal homepage: www.elsevier.com/locate/seppur

Catalytic reduction of bromate by Co-embedded N-doped carbon as a magnetic Non-Noble metal hydrogenation catalyst

Bing-Cheng Li [a], Hongta Yang [b], Eilhann Kwon [c], Duong Dinh Tuan [a], Ta Cong Khiem [a], Grzegorz Lisak [d,e], Bui Xuan Thanh [f], Farshid Ghanbari [g,*], Kun-Yi Andrew Lin [a,*]

[a] Department of Environmental Engineering & Innovation and Development Center of Sustainable Agriculture, National Chung Hsing University, 250 Kuo-Kuang Road, Taichung, Taiwan
[b] Department of Chemical Engineering, National Chung Hsing University, 250 Kuo-Kuang Road, Taichung, Taiwan
[c] Department of Environment and Energy, Sejong University, 209 Neungdong-ro, Gunja-dong, Gwangjin-gu, Seoul, Republic of Korea
[d] Residues and Resource Reclamation Centre, Nanyang Environment and Water Research Institute, Nanyang Technological University, Singapore 637141, Thailand
[e] School of Civil and Environmental Engineering, Nanyang Technological University, Singapore 639798, Thailand
[f] Faculty of Environment and Natural Resources, Ho Chi Minh City University of Technology, VNU-HCM, 268 Ly Thuong Kiet, District 10, Ho Chi Minh City, Viet Nam 700000, Thailand
[g] Department of Environmental Health Engineering, Abadan Faculty of Medical Sciences, Abadan, Iran

ARTICLE INFO

Keywords:
Bromate
Catalytic reduction
Bromide
Cobalt
N-doped carbon

ABSTRACT

While catalytic hydrogenation of bromate represents a useful technique for eliminating carcinogenic bromate, expensive noble-metal catalysts and excessive H_2 gas are usually required, impeding large-scale implementation of this technique. As borohydride is an alternative source for releasing H_2 in a more controllable way and non-noble metal catalysts (e.g., Co) can catalyze hydrolysis of borohydride to generate H_2, it is promising to employ Co and borohydride for hydrogenation of bromate. Moreover, it is even more practical to develop heterogeneous catalysts with magnetism for easier handle and recovery of catalysts. Therefore, the aim of this study is to develop such a magnetic heterogeneous catalyst for bromate reduction by using borohydride. Herein, a special Co-based catalyst is fabricated by transforming Co-substituted prussian blue analogue into Co-embedded N-doped carbon (Co@NC) composite through carbonization. Co@NC also exhibits a higher catalytic activity for reducing bromate than the commercial Co_3O_4 as Co@NC could accelerate hydrolysis of $NaBH_4$ to generate H_2 gas much faster. The activation energy (E_a) of bromate reduction by Co@NC is also much lower than the reported E_a. Co@NC could still completely remove bromate and reduce it to bromide under alkaline conditions, and Co@NC also exhibit a very high selectivity towards bromate reduction in the presence of other anions. Moreover, Co@NC could be also reused for multiple-cycles to continuously reduce bromate to bromide. These features demonstrate that Co@NC is certainly an advantageous and convenient heterogeneous catalyst for reducing bromate in water.

1. Introduction

As advanced oxidation technology (AOT) has been extensively employed for disinfection [1], numerous disinfection by-products (DBPs) would occur, and some of them are hazardous, posing serious threats on human health and ecology [2]. Among these hazardous DBPs, bromate (BrO_3^-) is particularly critical as bromate could be easily generated by oxidation of bromide ions, and bromate is proven to be carcinogenic as it is listed as a Group 2B substance by International Agency for Research on Cancer [3]. Therefore, World Health Organization has constrained its maximum concentration to 10 μg/L in drinking water due to its toxicity [3]. However, different levels of bromate have been also detected throughout the world. For instance, a study by Gunten et al. has been reported that the concentration of bromate in drinking water could reach to 40 μg/L in the United State [4], which is much higher than the bromate concentration reported in India (5.34 μg/L), Canada (6.11 μg/L) and Chile (8.8 ng/L) [5]. Another work by Husam and co-workers found that the concentrations of bromate detected in different water systems in Kuwait were 19.6 μg/L and 9.48 μg/L in tap water and saline brackish water, respectively [6].

Moreover, while ozonation is recognized as the typical AOT for causing the formation of bromate [7], recent studies have revealed

* Corresponding authors.
E-mail addresses: ghanbari.env@gmail.com (F. Ghanbari), linky@nchu.edu.tw (K.-Y.A. Lin).

https://doi.org/10.1016/j.seppur.2021.119320
Received 31 March 2021; Received in revised form 26 June 2021; Accepted 14 July 2021
Available online 17 July 2021
1383-5866/© 2021 Published by Elsevier B.V.

sulfate-radical-based AOT would also lead to the formation of bromate [8,9]. As these AOTs are widely-adopted in wastewater treatments and disinfection, it is critical and urgent to eliminate bromate from water to avoid its adverse effect.

Even though some studies have proposed to inhibit bromate formation during implementation of AOT [10], such a strategy is not satisfactory because bromate formation cannot be completely and effectively suppressed [11]. Thus, increasing attentions are paid to remove the resulting bromate from water through physio-chemical techniques, such as adsorption [12–14], filtration [15,16], membrane [17,18], etc. Even though these techniques could remove bromate, bromate actually is just transferred from aqueous phase to solid phase. Especially, while membrane processes seem a useful approach to remove bromate from solutions, highly-concentrated bromate would be produced [19]. Thus, alternative approaches must be taken and some studies attempted to reduce bromate back to bromide in order to lessen its toxicity [20–22].

Typically, bromate reduction can be achieved by using metal catalysts with H_2 gas to hydrogenate bromate. However, most of these studies require usage of noble metal catalysts (e.g., Pd and Ru), and continuous purge of H_2 gas [20,21]. For instance, Chen et al. developed a CoS_2 hollow sphere to reduce bromate in drinking water in the presence of H_2 gas as a reducing agent [23]. Besides, Li and co-workers prepared Pd nanoparticles supported on core-shell structured magnetite with polyaniline assisted with a continuous H_2 flow to perform the catalytic reduction of bromate [24]. Moreover, Sun's group synthesized a Pd catalyst supported on CeO_2 modified SBA-15 for catalytic hydrogenation reduction of bromate [25]. Though those studies have successfully reduced bromate to bromide, their sophisticated catalyst preparation procedure, usage of organic solvent and precious metal for preparing catalysts as well as H_2 gas-involved catalytic reduction certainly limit their widespread applications [26,27].

Therefore, non-noble-metal catalysts and a more controllable approach of introducing H_2 should be developed. As an alternative to H_2 gas, borohydrides are proven as safe, and convenient sources to release H_2 gas [28–30]. More importantly, H_2 release from borohydrides can be manipulated through catalyzing hydrolysis of borohydrides in water by non-noble-metal catalysts. Therefore, it would be advantageous to employ such a process for hydrogenation of bromate. Nevertheless, a few studies have been conducted to explore this process for bromate reduction [22,31,32]. Especially, it would be more promising and practical to develop heterogeneous catalysts with magnetism for easier handle and recovery after reactions. For instance, a nanoscale cobalt/carbon cage (NCC) was derived from ZIF-67 for catalyzing $NaBH_4$ to release H_2 for bromate reduction [32]. Thus, the aim of this study is to develop such a magnetic heterogeneous catalyst for bromate reduction by using borohydride as a reducing agent.

Since cobalt (Co) is validated as the most efficient non-noble-metal catalyst for hydrolysis of borohydride to generate H_2, a special Co-based catalyst is fabricated by embedding Co nanospheres onto a sheet-like carbonaceous substrate which is also doped with nitrogen for enhancing catalytic activities of Co through stabilizing effects [33,34]. Opposed to conventional fabrication of metal-immobilized carbon composites, a Co-substituted Prussian Blue Analogue (CoPBA) is adopted as a precursor, which is transformed to this Co-embedded N-doped carbon (Co@NC) composite through a simple carbonization. Through carbonization of CoPBA, Co ions of CoPBA are converted to Co^0 and Co_3O_4, whereas cyano groups of CoPBA are transformed to N-doped carbon. The resultant Co@NC comprised Co nanospheres well-distributed over N-doped carbon sheets to make active sites of Co species easier to expose to reactants, enabling Co@NC to be a promising catalyst for bromate reduction via catalyzed hydrolysis of borohydride.

2. Experimental

All reagents in this study were used as received without additional purification, and detailed information of reagents can be found in the supporting information. Preparation of Co@N-doped carbon (Co@NC) can be illustrated as shown in Fig. 1. Self-assembly of Co^{2+} and $Co(CN)_6^{3-}$ afforded CoPBA ($(Co_3[Co(CN)_6]_2$) which was then directly carbonized to produce Co@NC. The detailed procedure for fabricating Co@NC and characterization was given in the supporting information.

Catalytic reduction of bromate by Co@NC using $NaBH_4$ as a source of H_2 was evaluated through batch-type experiments. The experimental protocols can be then found in the supporting information. Removal efficiency for bromate and conversion efficiency for bromide were determined by the following equation:

$$q_t = \frac{v|C_0 - C_t|}{M} \quad (1)$$

where M (g) is the amount of Co@NC used in the reduction experiment and v (L) is the total volume of solution. For comparing removal efficiency for bromate and conversion efficiency of bromide, C_t, denoting the concentration of bromate (or bromide) at a given reaction time t, was expressed in mmol/L and so was C_0 (mmol/L), the initial concentration of bromate (or bromide). The q_e was used to express removal efficiency for bromate and conversion efficiency for bromide at equilibrium. An initial bromate concentration of 10 mg/L (i.e., 0.078 mM) was employed as this concentration has been extensively used as a model in published studies [23,35,36].

The temperature of 20 °C was particularly chosen as the standard temperature in the study to simulate the ambient temperature. The effect of temperature was investigated by varying temperature from 20 to 40, and 60 °C for further determining rate constants, and activation energy. For study the effect of co-existing anions on bromate reduction, bromate solution containing equivalent concentration (i.e., 10 mg/L) of those co-existing anions together was prepared to examine the joint effects of these anions. The concentration of Co concentration in water was measured using ICP-OES (Thermo Scientific Optima8300, USA). The concentration of DO was measured using a DO meter (YSI 5000).

3. Results and discussion

3.1. Characterization of Co@NC

As Co@NC was derived from CoPBA ($Co_3[Co(CN)_6]_2$) through carbonization, the morphology of CoPBA was visualized firstly in Fig. 2 (a), in which the as-prepared CoPBA was a group of nanoscale rounded particles. Its TEM image (Fig. 2(b)) also confirmed that $Co_3[Co(CN)_6]_2$ was comprised of many rounded nanoparticles that are consistent to the reported morphologies of PBA without addition of surfactants or citrates [37,38]. The corresponding crystalline structure of CoPBA was then displayed in Fig. S1, and the pattern was properly indexed to the reported X-ray diffraction (XRD) pattern of $Co_3[Co(CN)_6]_2$ [39–41], verifying the successful formation of CoPBA.

After CoPBA was carbonized to become Co@NC (Fig. 2(c)), the resultant Co@NC possessed a very distinct morphology as the rounded morphology of $Co_3[Co(CN)_6]_2$ had disappeared. Instead, the carbonized product of CoPBA exhibited many dark-colored nanospheres could be found on the light-colored substrate. A closer observation of Co@NC (Fig. 2(d)) further displays that the dark-colored particles were nanoscale with sizes ranging from 10 to 25 nm, and well-distributed over the light-colored substrate. This result indicates that CoPBA had been converted to form a nanocomposite material via carbonization to consist of nanospheres distributed over a sheet-like matrix.

To identify the composition of Co@NC, the XRD pattern of Co@NC was measured and is shown in Fig. 3(a), in which three noticeable peaks at 44.2°, 51.5° and 75.8° can be detected, and ascribed to crystallographic planes of (1 1 1), (2 0 0) and (2 2 0) of Co^0 (JCPDS# 15–0806), respectively. This suggests that cobalt formed and remained within Co@NC was in the form of Co^0. Nevertheless, several short peaks could be also noted at 31.2, 36.8, and 38.5°, corresponding to (2 2 0), (3 1 1),

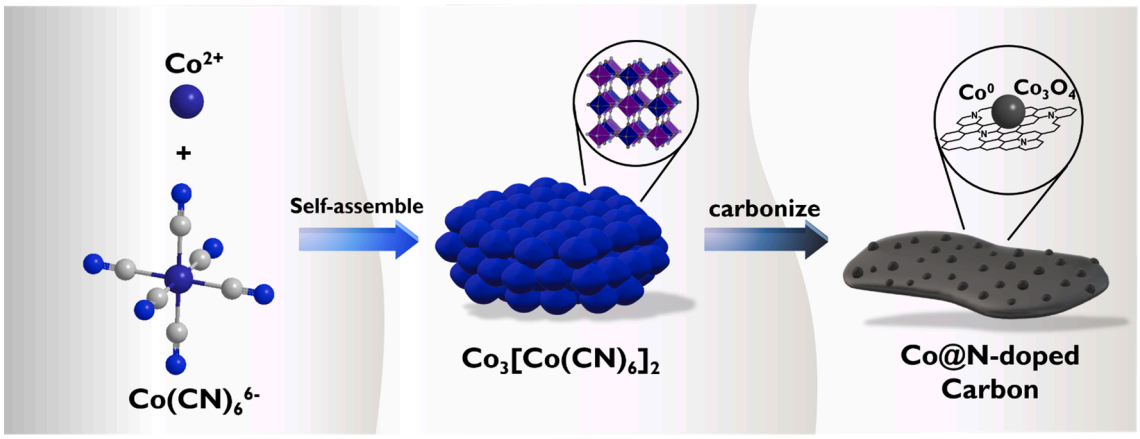

Fig. 1. Schematic illustration of preparation of Co@N-doped carbon (Co@NC).

and (2 2 2) planes of tricobalt tetraoxide (Co_3O_4) (JCPDS# 42–1467), demonstrating that a relatively low fraction of Co_3O_4 existed in Co@NC.

The presence of Co_3O_4 could be also verified by Raman spectroscopy. Fig. 3(b) displays a Raman spectrum of Co@NC, in which a series of bands at 192, 470, 510, and 682 Raman shift (cm^{-1}) were detected, and attributed to Co_3O_4 [42]. The peaks at 192, and 510 cm^{-1} were ascribed to the F_{2g} symmetry of Co_3O_4 [43], whereas the peak at 470 cm^{-1} corresponded to the E_g symmetry. Besides, the peak at 682 cm^{-1} could be assigned for the A_{1g} symmetry of Co_3O_4 [44,45]. Moreover, the conjugated carbon of Co@NC was also revealed in the Raman spectra. The peaks at 1350 and 1590 cm^{-1} could be attributed to the disordered structure carbon (i.e., the D band) and the graphitic carbon (i.e., the G band) of Co@NC, respectively. This demonstrates that the organic portion of CoPBA had been transformed into carbonaceous materials.

As reported in previous studies of carbonization of PBA into metal/carbon composites, the as-formed metal particles were present as dark-colored spheres whereas the light-colored substrate was a carbonaceous substrate [37]. Thus, the afore-mentioned features about Co@NC seemed to consist of the same configuration in which these dark-colored particles would be cobaltic particles embedded onto the carbonaceous matrix.

To further investigate surface chemistry of Co@NC, XPS analysis of Co@NC was conducted. Fig. 4(a) first shows C1s spectrum of Co@NC, which revealed three underlying peaks at 284.6, 285.3, and 287.5 eV, corresponding to C-C (sp^3), C-N, and C = O bonds, respectively [46,47], derived from N-doped carbon. Fig. 4(b) displays the core-level spectrum of Co2p, which could be deconvoluted to reveal multiple peaks. Specifically, the peaks at 780.2 and 797.2 eV were attributed to Co^{3+} [48,49], whereas the peaks at 781.8 and 798.6 eV corresponded to Co^{2+}. Nonetheless, the Co2p spectrum did not exhibit noticeable peaks of Co^0. This was possibly because the penetration depth of XPS analysis is very short and thus XPS is typically employed to analyze surficial chemistry of substrates. Co^0 on the surface of Co@NC might be been already oxidized to form Co_3O_4 [50–52]. Moreover, the N1s spectrum (Fig. 4(c)) was also deconvoluted to reveal two peaks at 397.6, and 399.6 eV, corresponding to pyridinic-N, and quaternary-N, respectively [53]. In particular, pyridinic N has been considered to be advantageous for stabilizing metal components [33,34].

Additionally, since Co@NC was derived from carbonization of CoPBA, thermogravimetric (TG) variation of CoPBA in N_2 was measured in Fig. 5(a). CoPBA started exhibiting weight loss from ca. 50 °C, and continued to lose weight until 200 °C possibly because of escape of gases or solvents in CoPBA. Next, a considerable weight loss occurred at 300 °C possibly due to carbonization of $Co(CN)_6$, and then weight remained steady until 600 °C at 50 wt%. This residual weight of CoPBA also indicated that the yield of conversion of CoPBA to Co@NC was ca. 50 wt%. On the other hand, the TG variation of Co@NC was also measured, and it did not exhibit any significant weight loss up to 600 °C, revealing a superior thermal stability of Co@NC.

On the other hand, since Co@NC was comprised of Co^0, making it a magnetic material, its saturation magnetization was then measured in Fig. 5(b). At ambient temperature, Co@NC can exhibit up to 130 emu/g, demonstrating a significantly high magnetism of Co@NC. The inset of Fig. 5(b) also revealed that Co@NC could be easily dispersed in solutions and collected by a magnet in solutions.

Furthermore, as catalytic bromate reduction by Co@NC occurs in aqueous solutions, it was important to realize surface charges of Co@NC in water as a function of pH. Fig. 5(c) displays that the surface charge of Co@NC was + 8 mV at pH = 3 and then gradually decreased at increasing pH. At pH = 7, the surface charge was ca. −17 eV, and further decreased to −48 eV at pH = 11, demonstrating that the surface charge of Co@NC was negatively-charged at most of pH values with a pH_{zpc} = ca. 3.7.

On the other hand, as Co@NC exhibited a very interesting morphology of sheet-supported Co, its textural properties were then determined by N_2 sorption isotherm. Fig. 5(c) displays that its N_2 sorption isotherm could be classified as the IUPAC type IV isotherm (IUPAC = International Union of Pure and Applied Chemistry) with a noticeable hysteresis loop, suggesting that Co@NC contained porous structures. The inset in Fig. 5(c) further confirmed that Co@NC contained mesopores and macropores. The BET surface area of Co@NC was then calculated as 21 m^2/g with a pore volume of 0.09 cm^3/g.

3.2. Catalytic bromate reduction using Co@NC in the presence of $NaBH_4$

Since bromate might be removed through adsorption, it was necessary to examine whether bromate could be removed simply by adsorption to Co@NC. Fig. 6(a) shows that when Co@NC alone was present, the concentration of bromate remained almost the same after 60 min without presence of any bromide, suggesting that bromate could not be removed and reduced by Co@NC via adsorption. On the other hand, we also investigated whether $NaBH_4$ alone could reduce bromate. Nevertheless, the reducing agent $NaBH_4$ was also tested to examine whether bromate could be removed and reduced by $NaBH_4$ alone. Nonetheless, when $NaBH_4$ alone was adopted, a very negligible amount of bromate could be removed and reduced to bromide. This demonstrated that even though $NaBH_4$ was a reducing agent, $NaBH_4$ itself could not effectively reduce bromate to bromide due to the fact that H_2 generation from self-hydrolysis of $NaBH_4$ was extremely slow.

Next, when Co@NC was combined with $NaBH_4$, the concentration of bromate rapidly decreased and became almost zero at 60 min. Correspondingly, bromide was also detected and the concentration of bromide quickly increased. Especially, the concentration of bromide (in mmol) occurred in the solution was almost comparable to the original

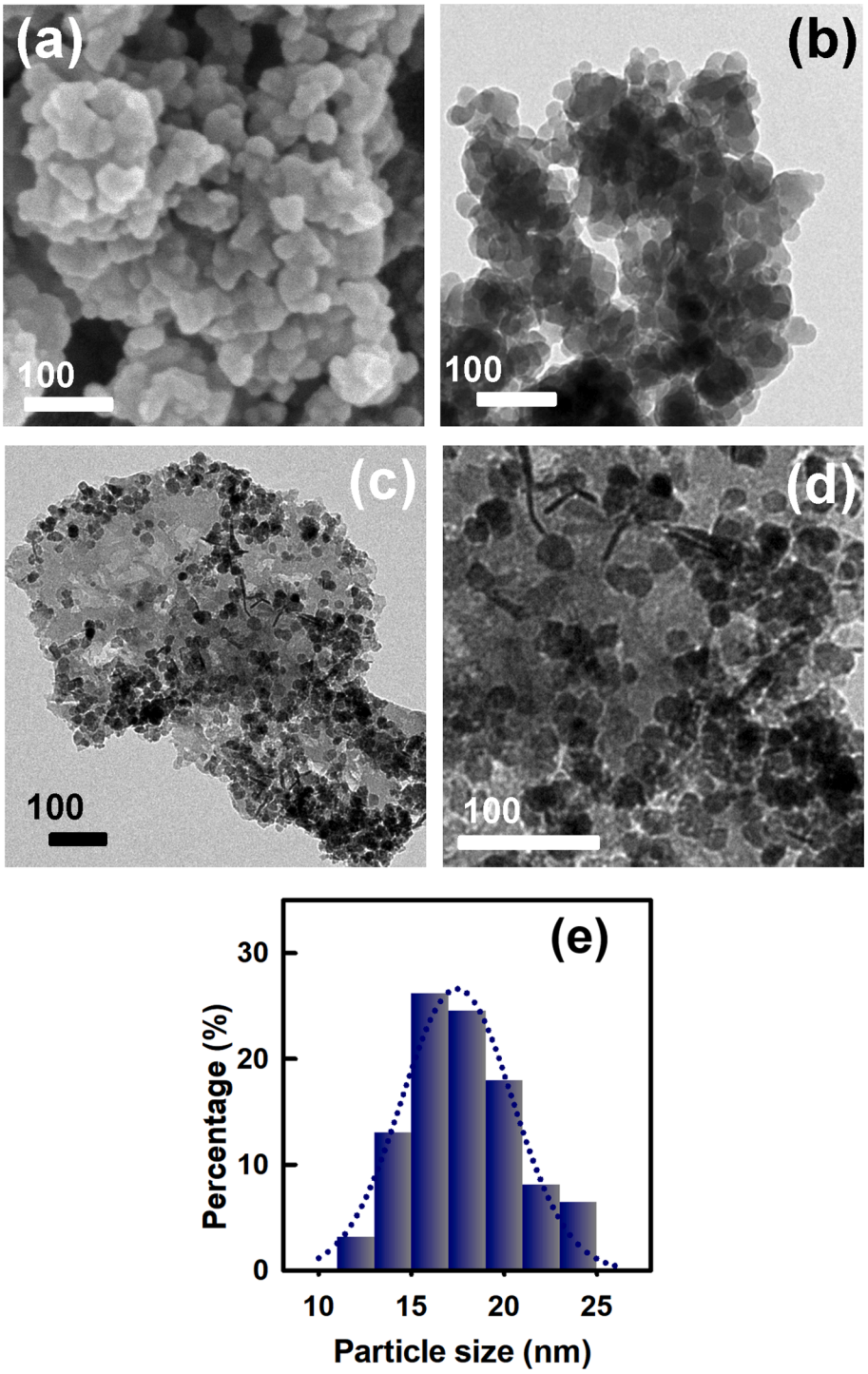

Fig. 2. (a) SEM and (b) TEM images of $Co_3[Co(CN)_6]_2$; (c), (d) TEM images of Co@NC at different magnifications; and (e) particle size distribution of nanospheres.

concentration of bromate (in mmol). This suggests that bromate was not only removed but also reduced successfully to bromide in the presence of Co@NC and $NaBH_4$. For comparing catalytic activities of Co@NC, the turnover frequency (TOF) of bromate reduction by Co@NC was also calculated based on the result in Fig. 6 as 0.42 h^{-1}. Since no TOFs of bromate reduction by Co-based catalysts has been reported in literatures, and most TOFs reported from studies of Pd-based catalysts, the TOF by Co@NC was then compared with TOFs by Pd-immobilized on carbonaceous supports as listed in Table S1. Even though Co@NC was a non-noble-metal catalyst, the TOF obtained by Co@NC was actually higher than Pd/AC, suggesting that Co@NC is certainly a useful non-noble-metal catalyst for bromate reduction.

As hydrolysis of $NaBH_4$ for generation of H_2 can be catalytically accelerated in the presence of metal catalysts via the following Eq.(2) [54,55]:

$$NaBH_4 + 2H_2O \rightarrow NaBO_2 + 2H_2 \quad (2)$$

the reaction of $NaBH_4$ with Co@NC would generate H_2 which would then react with bromate on the surface of Co@NC to become bromide and H_2O as follows (Eq. (3)):

$$BrO_3^- + 3H_2\ Br^- + 3H_2O \quad (3)$$

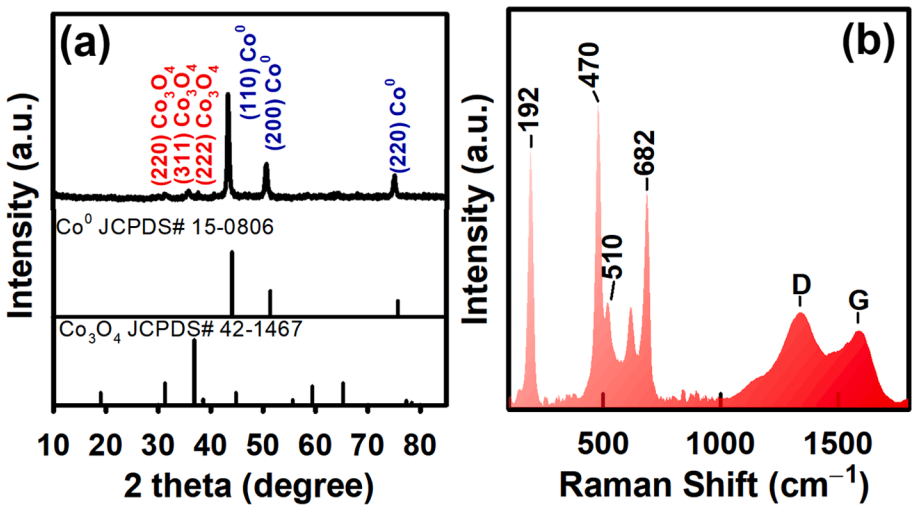

Fig. 3. Characteristics of Co@NC: (a) XRD pattern, (b) Raman spectrum.

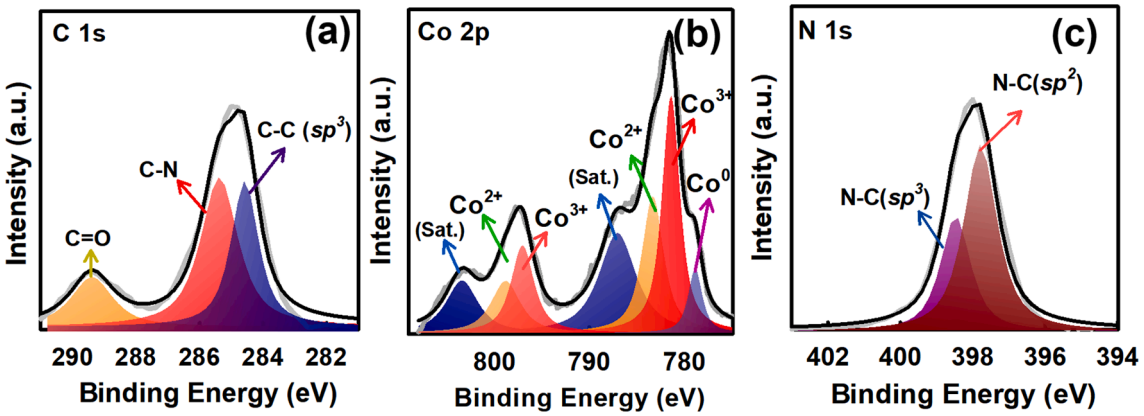

Fig. 4. Core-level XPS spectra of Co@NC: (a) C1s, (b) Co2p, and (c) N1s.

Fig. 6(b) displays H_2 generation by $NaBH_4$ in the presence of Co@NC; H_2 generation increase quickly along with the reaction time and reached an equilibrium after 20 min. The trend of H_2 generation seemed consistent to the trend of bromate reduction in Fig. 6(a). Bromate reduction by Co@NC with H_2 gas, and also H_2 gas alone was also evaluated and the results can be seen in the supporting information (Fig. S2) as follows. When Co@NC was combined with H_2 gas, the concentration of bromate could be noticeably removed, and bromide could be also detected (Fig. S2(c)). Even though bromate was not completely removed, this result certainly indicated that Co@NC can utilize H_2 gas to reduce bromate to bromide. Nevertheless, H_2 gas itself seemed incapable of removing and reducing bromate to bromide. This result is consistent to a reported study of using cobalt-based heterogeneous catalysts with H_2 gas to successfully reduce bromate to bromide [23]. These results suggested that removal of bromate by Co@NC + $NaBH_4$ would be related to the reaction expressed in Eq.(3), which could occur through a few possible mechanisms [56].

In the first mechanism, bromate might still transitorily stay on the surface of Co@NC, and encounter with H_2 molecules derived from Co@NC + $NaBH_4$ to transform into bromide as the path #1 in Fig. 7. Additionally, since Co@NC contained Co^0, and Co^{2+}, these Co species would donate electrons to bromate and convert it to bromide, while these Co species would be reduced back to their original reductive states by H_2 [56] as the path #2 in Fig. 7.

While Co@NC was certainly capable of catalyzing hydrolysis of $NaBH_4$ and further reducing bromate to bromide, it would be necessary to further compare Co@NC with other cobalt catalysts. To this end, the commercial Co_3O_4 nanoparticle (NPs) (Fig. S3) was employed as a reference catalyst as Co_3O_4 is a well-proven catalyst to catalyze hydrolysis of $NaBH_4$, and thus was further used for bromate reduction here. Fig. 6(c) and (d) display that the concentration of bromate also noticeably decreased along with the reaction time, and bromide could be also detected correspondingly. This validates that Co_3O_4 was also capable of reducing bromate to bromide; nevertheless, the removal efficiency for bromate by Co_3O_4 NP was significantly lower than that by Co@NC. To further elucidate the possible reason behind the phenomenon, H_2 generation from $NaBH_4$ catalyzed by Co_3O_4 NP was also tested in Fig. 6(b). Interestingly, H_2 generation was certainly accelerated by Co_3O_4 NP, confirming that Co_3O_4 NP could catalyze hydrolysis of $NaBH_4$. Nonetheless, the H_2 generation amount and rate by Co_3O_4 NP were both much lower than those by Co@NC, thereby leading to the lower removal efficiency for bromate by Co_3O_4 NP. This comparison further validated that bromate reduction by Co@NC was certainly involved with H_2 generation by $NaBH_4$, and H_2 would then react with bromate and reduce cobalt species to convert bromate to bromide. Such a comparison also demonstrated that Co@NC was an advantageous and promising Co-based catalyst for reducing bromate in the presence of $NaBH_4$.

3.3. Effect of Co@NC dosage on bromate reduction

As Co@NC played a critical role for catalyzing hydrolysis of $NaBH_4$ and bromate reduction, it would be essential to further examine the

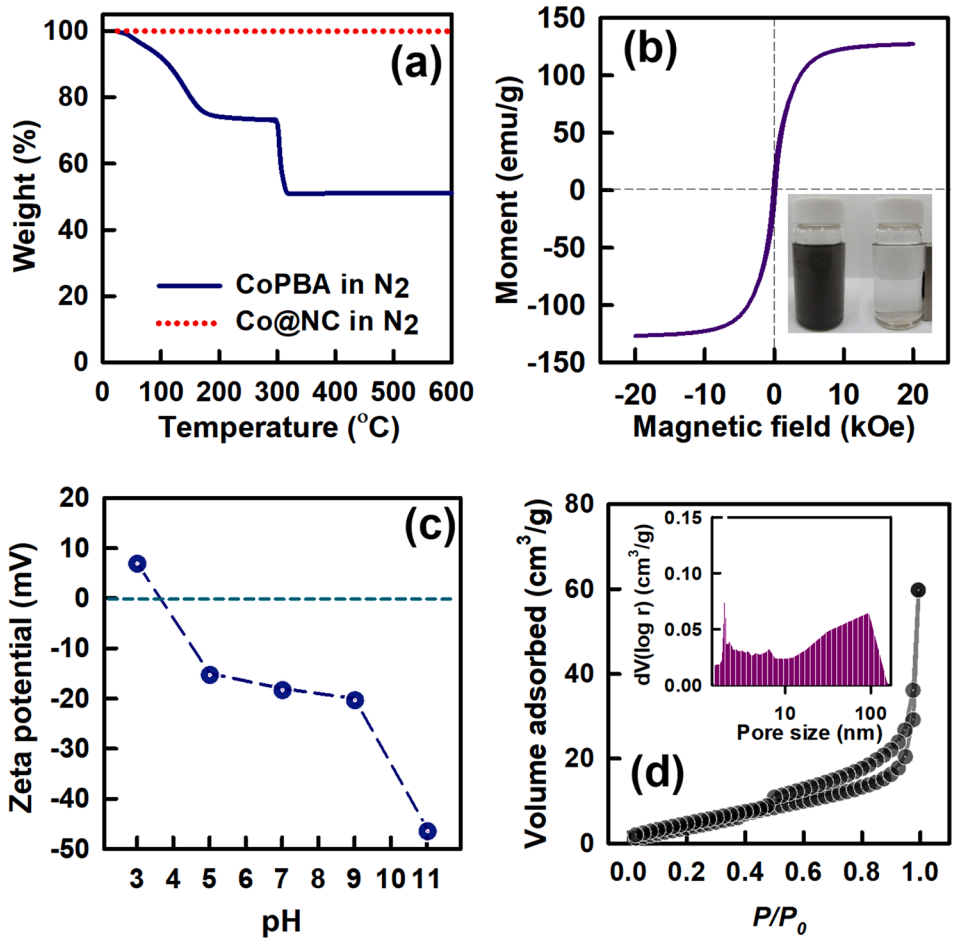

Fig. 5. Physical properties of Co@NC: (a) thermal stability, (b) saturation magnetization at ambient temperature, (c) zeta potentials as a function of pH, and (d) N_2 sorption isotherm and pore size distribution.

effect of Co@NC dosage on bromate reduction by Co@NC + $NaBH_4$. To this end, the dosage of Co@NC was varied from 250 to 500, and then 750 mg/L for bromate reduction as shown in Fig. 6(c).

When the dosage of Co@NC increased from 250 to 500 mg/L, the complete removal of bromate was achieved within a shorter time (i.e., 30 min). Correspondingly, the full conversion of bromate to bromide was also achieved within a much shorter time. Such an enhancing effect of higher Co@NC dosage became even more pronounced as the dosage of Co@NC further increased to 750 mg/L as the full conversion of bromate to bromide was completed in 15 min. This result demonstrates that when more active sites (i.e., Co species in Co@NC) were present, bromate reduction could be significantly accelerated.

On the other hand, even though a higher dosage of Co@NC could enhance bromate reduction through accelerating the reaction, it would be interesting to further calculate removal efficiency (q_t) of bromate in terms of molecules of bromate removed per gram of catalyst (mmol/g). Fig. 8(a) displays that while the higher dosages of Co@NC could considerably accelerate bromate reduction, their corresponding removal efficiencies (q_t) were in fact noticeably lower than that at a lower dosage of Co@NC. Fig. 8(b) also indicates that the conversion efficiency for bromide by a lower dosage of Co@NC was substantially higher than those by the higher dosages of Co@NC. This result demonstrates that while bromate reduction can be accelerated by the more active sites from a higher Co@NC dosage, each activate site might be not fully utilized to contribute to catalytic bromate reduction. In view of respective advantages of lower and higher dosages of Co@NC, the dosage of 500 mg/L was then selected for further investigating other effects on bromate reduction by Co@NC + $NaBH_4$.

3.4. Effect of temperature on bromate reduction

As temperature is an important factor to catalytic reduction and hydrolysis of $NaBH_4$ [57–59], the effect of temperature on bromate reduction was then investigated. Fig. 9(a) shows the removal efficiencies for bromate (q_t) by Co@NC + $NaBH_4$ at 20, 40, and 60 °C.

At increasing temperatures, bromate removal proceeded much faster to its equilibrium state, indicating that the higher temperature would enhance bromate reduction particularly in terms of degradation kinetics. To further quantify the kinetics for bromate removal in terms of removal efficiencies (q_t), the pseudo first order rate law was then adopted as follows:

$$q_t = q_e(1 - e^{-k_1 t}) \quad (4)$$

where q_t is the removal efficiency for bromate at time t, qe is the removal efficiency for bromate at equilibrium, and k_1 is the rate constant (min-1). The corresponding k_1 values at 20, 40, and 60 °C were displayed in the inset of Fig. 9(a), and k1 increased from 0.126 to 0.222, and 0.381 min^{-1} as temperature was raised up from 20 to 40 and 60 °C, respectively. Similarly, the same feature can be observed in the case of conversion efficiency (q_t) for bromide at different temperatures in Fig. 9(b). As the temperature increased, the conversion efficiency (q_t) for bromide also proceeded faster. The corresponding k_1 increased from 0.126 to 0.199, and 0.290 min^{-1} as temperature was raised up from 20 to 40 and 60 °C, respectively. These results ascertained the enhancing effect of higher temperatures.

Furthermore, since the rate constants increased along with the reaction temperature, the relationship of rate constant of bromate reduc-

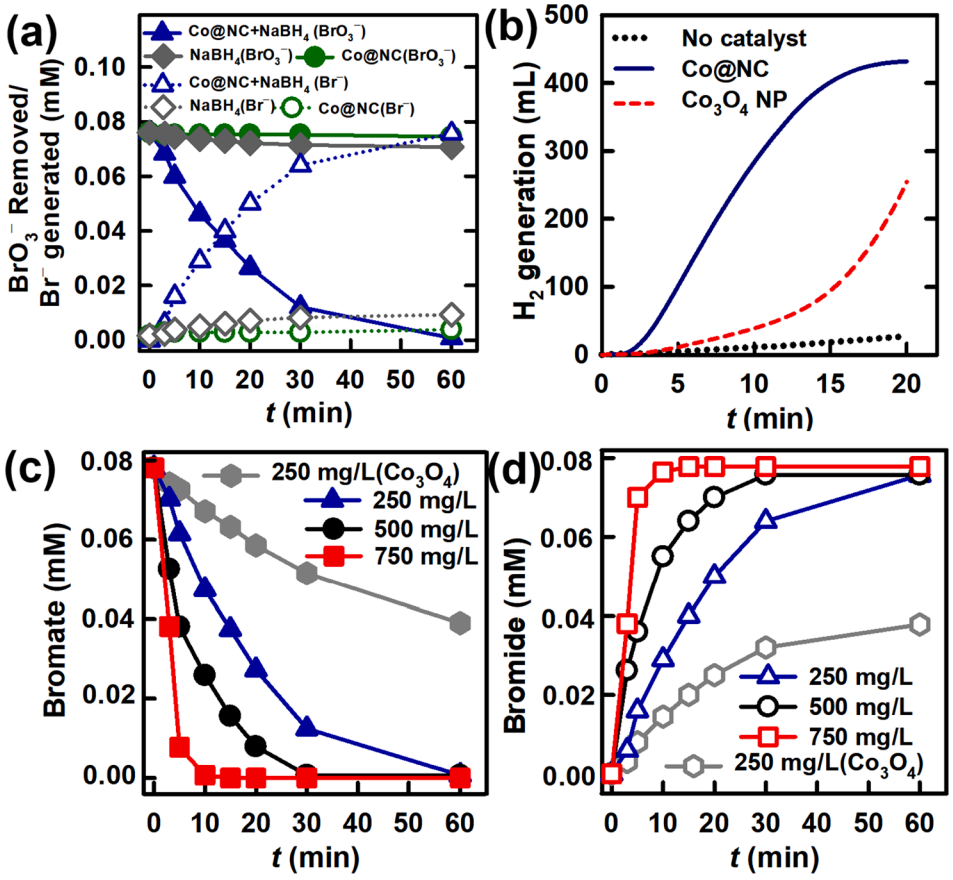

Fig. 6. (a) removal of bromate (bromate = 10 mg/L = 0.078 mM, T = 20 °C) and (b) H_2 evolution from $NaBH_4$ by Co@NC and the commercial Co_3O_4 NP ($NaBH_4$ = 500 mg/L, catalyst = 500 mg/L, T = 20 °C); effect of catalyst dosage on (c) removal of bromate, and (d) generation of bromide (bromate = 0.078 mM, T = 20 °C).

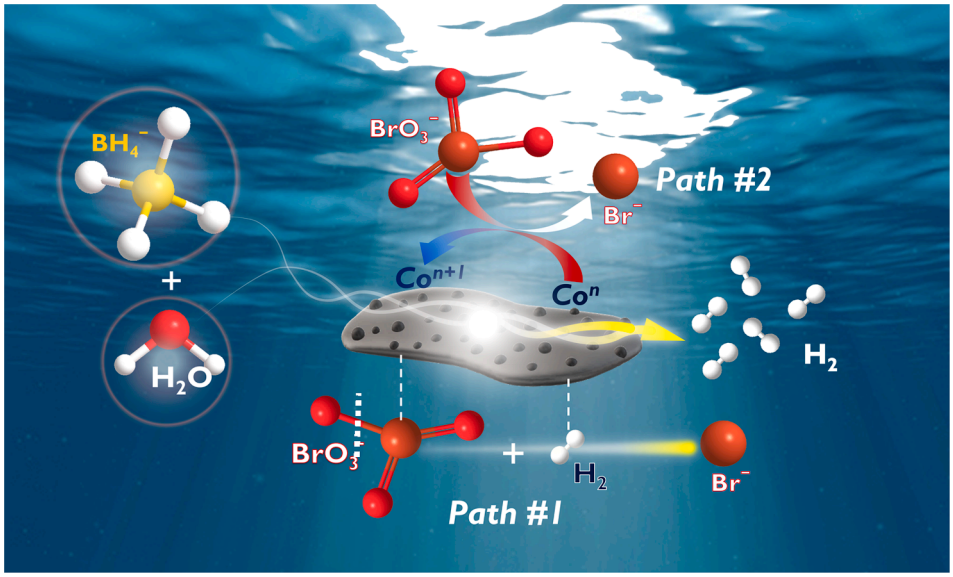

Fig. 7. Proposed mechanisms for bromate reduction to bromide by Co@NC in the presence of $NaBH_4$.

tion and temperature was then correlated through the Arrhenius equation as follows (Eq.(5)):

$$\ln k_1 = \ln A - E_a/RT \quad (5)$$

where *Ea* represents the activation energy (kJ/mol) for the bromate reduction, *A* represents the temperature-independent factor (g/mg/min); *R* is the universal gas constant and *T* is the solution temperature in Kelvin (K). A plot of ln *k1* versus 1/*T* was displayed in Fig. S4 (the supporting information). The data points are properly fitted by the linear regression (R2 = 0.990), suggesting that the kinetics of bromate reduction can be correlated to temperature via by the Arrhenius equation. The corresponding *Ea* was then calculated as 22.4 kJ/mol, which

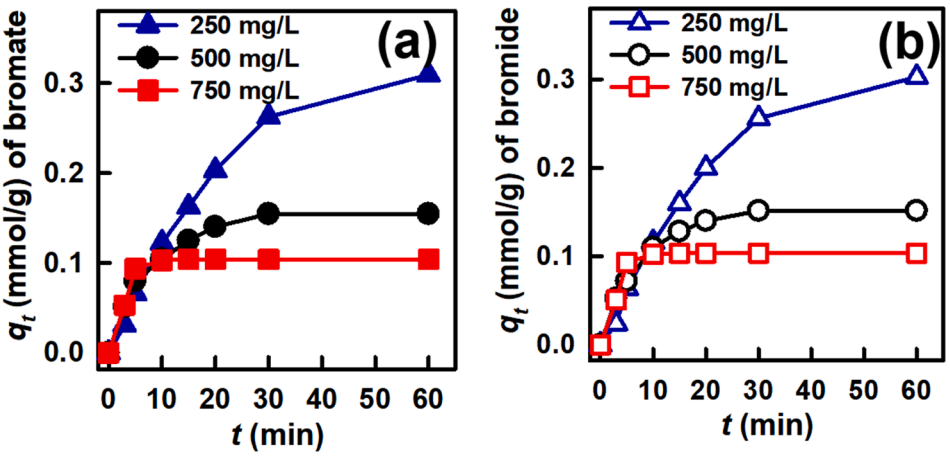

Fig. 8. Effect of Co@NC dosage on (a) removal efficiency of bromate (mmol/g) and (b) conversion efficiency of bromide (mmol/g) using Co@NC (bromate = 0.078 mM, catalyst = 500 mg/L, $NaBH_4$ = 500 mg/L, T = 20 °C).

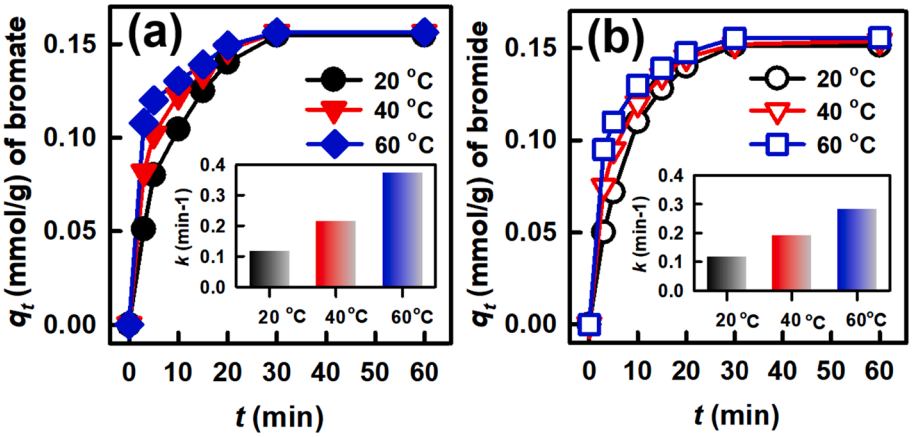

Fig. 9. Effect of temperature on (a) removal efficiency of bromate (mmol/g) and (b) conversion efficiency of bromide (mmol/g) using Co@NC (bromate = 0.078 mM, catalyst = 500 mg/L, $NaBH_4$ = 500 mg/L, T = 20 °C).

was much lower than the reported values (~40 kJ/mol) of bromate reduction using other catalysts [32], demonstrating the promising advantage of Co@NC.

3.5. Effects of pH and co-existing anions on bromate reduction

Since bromate reduction occurs in aqueous solutions, pH values shall influence reductive processes of bromate. Thus, the effect of pH was further investigated by changing bromate solutions to become acidic,

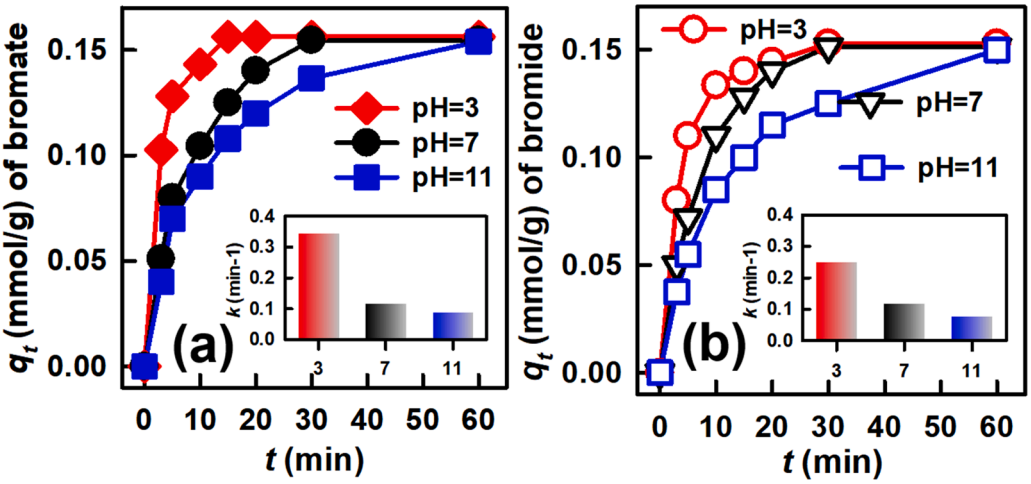

Fig. 10. Effect of pH on (a) removal efficiency of bromate (mmol/g) and (b) conversion efficiency of bromide (mmol/g) using Co@NC (bromate = 0.078 mM, catalyst = 500 mg/L, $NaBH_4$ = 500 mg/L, T = 20 °C).

neutral and alkaline conditions. Fig. 10(a) shows the removal efficiencies for bromate at pH = 3, 7, and 11, revealing that bromate reduction was considerably influenced by the initial pH of bromate solution. Specifically, when the solution was acidic at pH = 3, bromate reduction proceeded much faster than that at pH = 7, and reached the equilibrium (qe) just in 15 min.

The corresponding k_1 was 0.35 min^{-1}, which was much higher than k_1 of 0.126 min^{-1} at pH = 7, suggesting the acidic condition seemed to facilitate bromate reduction. In contrast, at pH = 11, bromate reduction proceeded noticeably slower with k1 of 0.098 min^{-1} while bromate could be still completely removed. Similar trends can be observed in the case of conversion efficiency for bromide at different pH in Fig. 10(b). At pH = 3, q_t for bromide also proceeded much quicker with a k_1 of 0.255 min^{-1} which was also substantially higher than that at pH = 7 (0.126 min^{-1}). However, when pH became 11, the corresponding k_1 also dropped significantly to 0.090 min^{-1}.

These results revealed that the acidic condition would facilitate bromate reduction, while the alkaline condition would hinder the reductive process. As illustrated in Fig. 7, the mechanism of bromate reduction via the path #2 would be achieved through reactions between bromate anions presented on the surface of Co@NC and H_2. Since the surface of Co@NC would become positively-charged owing to accumulation of H^+ at pH = 3, the electrostatic attraction between bromate anions and Co@NC would be strengthened and facilitate approach of bromate towards Co@NC. On the contrary, the alkaline condition would make the surface of Co@NC more negatively-charged as displayed in Fig. 5(c), causing stronger electrostatic revulsion between bromate anions and Co@NC, constraining approach of bromate towards Co@NC and limiting reductive reactions [60,61]. Besides, OH^- anions would compete with BH_4^- anions to occupy the surfaces of Co@NC, diminishing the contact between active sites and BH_4^- anions, then lowering the mass transfer in catalytic system [62,63], thus subsequently decreasing the hydrogen generation rate and bromate reduction efficiency from Co@NC + $NaBH_4$ system.

In addition, as bromate may co-exist with other species, especially anions such as nitrate, phosphate and sulfate, it would be critical to investigate whether these typical anions would seriously influence bromate reduction by Co@NC + $NaBH_4$. Before evaluating the effect of different anions, bromate solution containing equivalent concentration (i.e., 10 mg/L) of those co-existing anions was firstly prepared. Fig. 11 (a) shows removal efficiency for bromate in the absence and presence of co-existing anions.

Interestingly, bromate was still completely and quickly removed in the presence of co-existing anions; the corresponding k1 (as seen in the inset) was only slightly lower than that obtained in the absence of co-existing anions. The similar result can be observed in the case of conversion efficiency for bromide in Fig. 11(b) as bromate could be still completely converted and reduced to bromide. The corresponding k_1 was also very comparable to that obtained in the absence of co-existing anions. Interestingly, Fig. 11(a) also shows that these co-exist anions (nitrate, phosphate and sulfate) were almost not removed and adsorbed by Co@NC. The results validate that Co@NC + $NaBH_4$ can exhibit high selectivities towards bromate anions and effectively convert bromate to bromide even in the presence of other anions.

On the other hand, as dissolved oxygen (DO) may cause adverse effect to the reduction of bromate as illustrated in literature [64,65], the effect of different DO concentrations on bromate reduction using Co@NC + $NaBH_4$ had been also investigated. When DO was increased from 5 (the original case) to 15 mg/L (with additional purge of O_2), bromate reduction was slightly influenced as bromate was incompletely eliminated even though the reduced bromate was still converted to bromide (Fig. S5(c)). This result suggests that the reduction of bromate using Co@NC + $NaBH_4$ was slightly inhibited with high concentrations of DO. Similarly, Xiao et al. found that higher DO concentrations inhibited bromate reduction efficiencies of a sulfite/Fe(II) system [35]. Besides, Nawaz and co-workers also reported that DO caused a negative effects to bromate removal using UV-254/sulfite [66]. This information had been added in the main text. Please see the revised manuscript.

3.6. Recyclability of Co@NC for bromate reduction

As Co@NC was proposed as a magnetic heterogeneous catalyst for easier recovery and reuse, it would be necessary to further examine its recyclability. Fig. 12 displays multi-cyclic removal efficiencies for bromate and conversion efficiencies for bromide at equilibrium over 6 cycles by reusing Co@NC without any regeneration treatments. In the consecutive cycles, bromate could be consistently and completely removed and reduced to bromide without significant changes. This indicates that the used Co@NC could still exhibit robust catalytic activities towards bromate reduction. Moreover, the used Co@NC was also examined for its crystalline structure (Fig. 12(b)) which was very comparable to that of pristine Co@NC, demonstrating that Co@NC was a reusable and stable catalyst for reducing bromate. The concentration of Co^{2+} from Co@NC for multiple bromate reduction cycles had been measured as 0.015 mg/L using ICP-MS, which is much lower than the initial concentration of Co@NC (i.e., 500 mg/L) as well as the standard Co ion permission in drinking water (100 μg/L) by Environmental Protection Agency (EPA), USA, validating that Co@NC was a stable and durable catalyst.

For comparison, numerous studies have also employed heterogeneous catalysts for catalytic reduction of bromate using $NaBH_4$. A previous study employed an iron MOF (i.e., MIL-88A) and a cobalt MOF (i.e., ZIF-67) for catalyzing $NaBH_4$ to produce hydrogen in situ and reduce bromate [67]. Moreover, a nanoscale cobalt/carbon cage (NCC) has

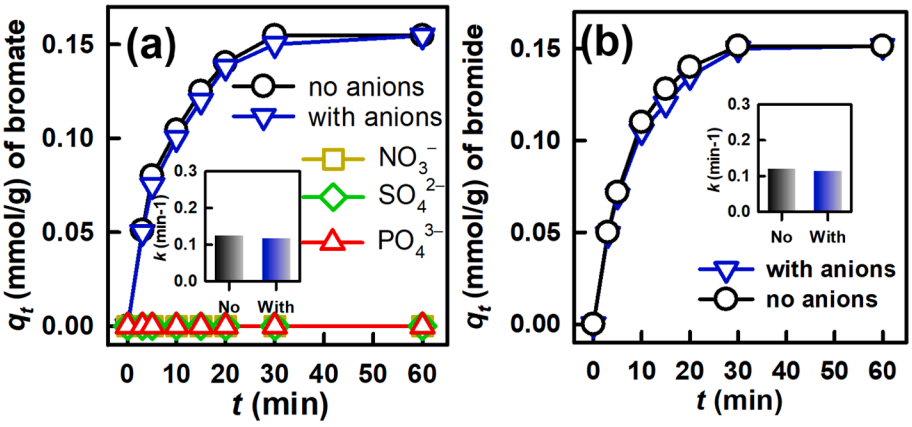

Fig. 11. Effect of anions on (a) removal efficiency of bromate (mmol/g) and (b) conversion efficiency of bromide (mmol/g) using Co@NC (bromate = 0.078 mM, catalyst = 500 mg/L, $NaBH_4$ = 500 mg/L, T = 20 °C).

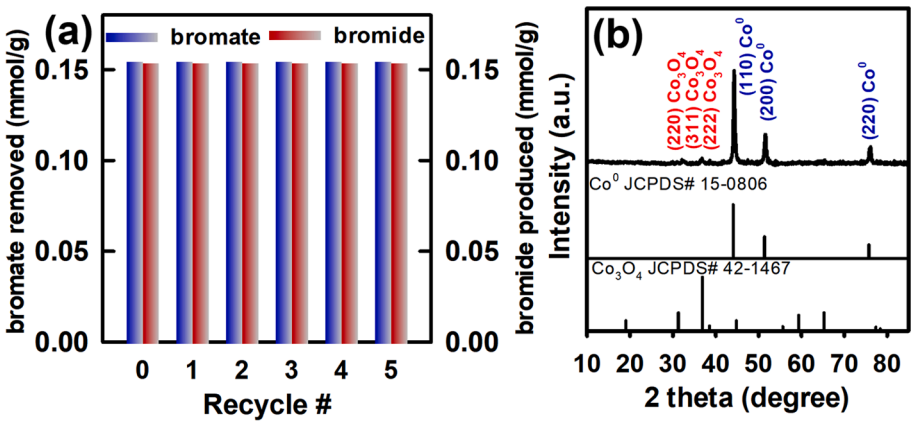

Fig. 12. (a) recyclability of Co@NC for reduction of bromate to bromide (bromate = 0.078 mM, catalyst = 500 mg/L, $NaBH_4$ = 500 mg/L, T = 20 °C), and (b) XRD pattern of used Co@NC.

been also developed for bromate reduction in the presence of $NaBH_4$ [32]. Besides, a recent work by Nurlan and co-workers fabricated a Ni-MOF and used it to accelerate the hydrolysis of $NaBH_4$ to remove aqueous bromate [31]. Nevertheless, most of the reported catalysts did not possess magnetism property, reducing their reusable capabilities. In contrast, Co@NC was prepared via a simple method and exhibited high catalytic activity for reducing bromate. Especially, Co@NC also possessed strong magnetism, making it superior reusability for multiple bromate reduction cycles.

4. Conclusion

In this study, a magnetic Co-embedded N-doped carbon composite (Co@NC) was developed from direct carbonization of CoPBA to serve as a magnetically-controllable heterogeneous catalyst for bromate reduction in the presence of $NaBH_4$. Through carbonization of CoPBA, Co ions of CoPBA were converted to Co^0 and Co_3O_4, whereas cyano groups of CoPBA were transformed to N-doped carbon to stabilize catalytic characteristics of Co species. The resultant Co@NC comprised Co nanospheres well-distributed over N-doped carbon sheets to make active sites of Co species easier to expose to reactants. While Co@NC and $NaBH_4$ could not remove and reduce bromate individually, the combination of Co@NC and $NaBH_4$ could rapidly and completely reduce bromate to bromide. Co@NC could also exhibit higher catalytic activity for reducing bromate than the commercial Co_3O_4 NP as Co@NC could accelerate hydrolysis of $NaBH_4$ to generate H_2 gas much faster. More importantly, three mechanisms for reducing bromate by Co@NC + $NaBH_4$ were proposed on the basis of interactions of bromate, Co@NC and resulting H_2 gas. The E_a of bromate reduction by Co@NC was also much lower than the reported E_a in literature. Co@NC could still completely remove bromate and reduce it back to bromide under alkaline conditions, and Co@NC also exhibit a very high selectivity towards bromate reduction even in the presence of other anions. Moreover, Co@NC could be also reused for multiple-cycles to continuously reduce bromate to bromide. These features demonstrate that Co@NC was certainly an advantageous and convenient heterogeneous catalyst for reducing bromate in water.

CRediT authorship contribution statement

Bing-Cheng Li: Data curation, Writing - original draft. **Hongta Yang:** Data curation. **Eilhann Kwon:** Data curation, Visualization, Investigation. **Duong Dinh Tuan:** Writing - review & editing. **Ta Cong Khiem:** Visualization, Investigation. **Grzegorz Lisak:** Data curation, Visualization. **Bui Xuan Thanh:** Data curation, Visualization, Investigation. **Farshid Ghanbari:** Writing - original draft, Investigation. **Kun-Yi Andrew Lin:** Data curation, Writing - original draft.

Declaration of Competing Interest

The authors declare that they have no known competing financial interests or personal relationships that could have appeared to influence the work reported in this paper.

Acknowledgement

This work is supported by the Ministry of Science and Technology (MOST)(110-2636-E-005-003-), Taiwan, and financially supported by the "Innovation and Development Center of Sustainable Agriculture" from The Featured Areas Research Center Program within the framework of the Higher Education Sprout Project by the Ministry of Education (MOE), Taiwan. The authors gratefully acknowledge the use of SQUID000200 of MOST110-2731-M-006-001 belonging to the Core Facility Center of National Cheng Kung University.

Appendix A. Supplementary material

Supplementary data to this article can be found online at https://doi.org/10.1016/j.seppur.2021.119320.

References

[1] I.A. Ike, Y. Lee, J. Hur, Impacts of advanced oxidation processes on disinfection byproducts from dissolved organic matter upon post-chlor(am)ination: A critical review, Chem Eng J 375 (2019), 121929.
[2] V.K. Sharma, R. Zboril, T.J. McDonald, Formation and toxicity of brominated disinfection byproducts during chlorination and chloramination of water: A review, J Env Sci Health, Part B 49 (2014) 212–228.
[3] U. Pinkernell, U. von Gunten, Bromate Minimization during Ozonation: Mechanistic Considerations, Environ Sci Technol 35 (2001) 2525–2531.
[4] U. von Gunten, Ozonation of drinking water: Part II, Disinfection and by-product formation in presence of bromide, iodide or chlorine, Water Res 37 (2003) 1469–1487.
[5] C. Raúl, U.-J. Kim, K. Kannan, Occurrence and human exposure to bromate via drinking water, fruits and vegetables in Chile, Chemosphere 228 (2019) 444–450.
[6] H.F. Alomirah, S.F. Al-Zenki, M.C. Alaswad, N.A. Alruwaih, Q. Wu, K. Kannan, Elevated concentrations of bromate in Drinking water and groundwater from Kuwait and associated exposure and health risks, Environ Res 181 (2020), 108885.
[7] M.M. Huber, S. Canonica, G.-Y. Park, U. von Gunten, Oxidation of Pharmaceuticals during Ozonation and Advanced Oxidation Processes, Environ Sci Technol 37 (2003) 1016–1024.
[8] K. Liu, J. Lu, Y. Ji, Formation of brominated disinfection by-products and bromate in cobalt catalyzed peroxymonosulfate oxidation of phenol, Water Res 84 (2015) 1–7.
[9] Z. Li, Z. Chen, Y. Xiang, L. Ling, J. Fang, C. Shang, D.D. Dionysiou, Bromate formation in bromide-containing water through the cobalt-mediated activation of peroxymonosulfate, Water Res 83 (2015) 132–140.
[10] G.L. Amy, M.S. Siddiqui, A.R. Foundation, Strategies to Control Bromate and Bromide, AWWA Research Foundation and American Water Works Association, 1999.
[11] R. Song, R. Minear, P. Westerhoff, G. Amy, Bromate Formation and Control During Water Ozonation, Environ Technol 17 (1996) 861–868.

[12] A. Bhatnagar, Y. Choi, Y. Yoon, Y. Shin, B.-H. Jeon, J.-W. Kang, Bromate removal from water by granular ferric hydroxide (GFH), J Hazard Mater 170 (2009) 134–140.
[13] J.A. Wiśniewski, M. Kabsch-Korbutowicz, Bromate removal in the ion-exchange process, Desalination 261 (2010) 197–201.
[14] Y. Yang, Z. Zheng, W. Ji, M. Yang, Q. Ding, X. Zhang, The study of bromate adsorption onto magnetic ion exchange resin: Optimization using response surface methodology, Surf Interfaces 17 (2019), 100385.
[15] K. Listiarini, J.T. Tor, D.D. Sun, J.O. Leckie, Hybrid coagulation–nanofiltration membrane for removal of bromate and humic acid in water, J Membr Sci 365 (2010) 154–159.
[16] S. C.S, A. C.T, U.K. Aravind, Detection of bromate in packaged drinking water and its removal using polyelectrolyte multilayer membranes, Environ Qual Manage 30 (2021) 101–112.
[17] C.T. Matos, S. Velizarov, M.A.M. Reis, J.G. Crespo, Removal of Bromate from Drinking Water Using the Ion Exchange Membrane Bioreactor Concept, Environ Sci Technol 42 (2008) 7702–7708.
[18] Rejection of Bromide and Bromate Ions by a Ceramic Membrane, Environmental Engineering Science, 29 (2012) 1092-1096.
[19] M. Moslemi, S.H. Davies, S.J. Masten, Rejection of Bromide and Bromate Ions by a Ceramic Membrane, Environ Eng Sci 29 (2012) 1092–1096.
[20] H. Chen, Z. Xu, H. Wan, J. Zheng, D. Yin, S. Zheng, Aqueous bromate reduction by catalytic hydrogenation over Pd/Al2O3 catalysts, Appl Catal B 96 (2010) 307–313.
[21] Y. Marco, E. García-Bordejé, C. Franch, A.E. Palomares, T. Yuranova, L. Kiwi-Minsker, Bromate catalytic reduction in continuous mode using metal catalysts supported on monoliths coated with carbon nanofibers, Chem Eng J 230 (2013) 605–611.
[22] D.-W. Cho, G. Kwon, Y.S. Ok, E.E. Kwon, H. Song, Reduction of Bromate by Cobalt-Impregnated Biochar Fabricated via Pyrolysis of Lignin Using CO2 as a Reaction Medium, ACS Appl Mater Interfaces 9 (2017) 13142–13150.
[23] Y. Chen, W. Yang, S. Gao, Y. Gao, C. Sun, Q. Li, Catalytic reduction of aqueous bromate by a non-noble metal catalyst of CoS2 hollow spheres in drinking water at room temperature, Sep Purif Technol 251 (2020), 117353.
[24] M. Li, X. Zhou, J. Sun, H. Fu, X. Qu, Z. Xu, S. Zheng, Highly effective bromate reduction by liquid phase catalytic hydrogenation over Pd catalysts supported on core-shell structured magnetites: Impact of shell properties, Sci Total Environ 663 (2019) 673–685.
[25] J. Sun, J. Zhang, H. Fu, H. Wan, Y. Wan, X. Qu, Z. Xu, D. Yin, S. Zheng, Enhanced catalytic hydrogenation reduction of bromate on Pd catalyst supported on CeO2 modified SBA-15 prepared by strong electrostatic adsorption, Appl Catal B 229 (2018) 32–40.
[26] T.E. Crozier, S. Yamamoto, Solubility of hydrogen in water, sea water, and sodium chloride solutions, J. Chem. Eng. Data 19 (1974) 242–244.
[27] J.L. Cerrillo, A.E. Palomares, A Review on the Catalytic Hydrogenation of Bromate in Water Phase, Catalysts 11 (2021) 365.
[28] S. Özkar, M. Zahmakıran, Hydrogen generation from hydrolysis of sodium borohydride using Ru(0) nanoclusters as catalyst, J Alloy Compd 404–406 (2005) 728–731.
[29] Y. Kojima, K.-I. Suzuki, K. Fukumoto, M. Sasaki, T. Yamamoto, Y. Kawai, H. Hayashi, Hydrogen generation using sodium borohydride solution and metal catalyst coated on metal oxide, Int J Hydrogen Energy 27 (2002) 1029–1034.
[30] B.H. Liu, Z.P. Li, A review: Hydrogen generation from borohydride hydrolysis reaction, J Power Sources 187 (2009) 527–534.
[31] N. Nurlan, A. Akmanova, S. Han, W. Lee, Enhanced reduction of aqueous bromate by catalytic hydrogenation using the Ni-based Metal-organic framework Ni(4,4′-bipy)(1,3,5-BTC) with NaBH4, Chem Eng J 414 (2021), 128860.
[32] K.-Y.A. Lin, S.-Y. Chen, Catalytic Reduction of Bromate Using ZIF-Derived Nanoscale Cobalt/Carbon Cages in the Presence of Sodium Borohydride, Acs Sustain Chem Eng 3 (2015) 3096–3103.
[33] W. Ma, N. Wang, Y. Du, T. Tong, L. Zhang, K.-Y. Andrew Lin, X. Han, One-step synthesis of novel Fe3C@nitrogen-doped carbon nanotubes/graphene nanosheets for catalytic degradation of Bisphenol A in the presence of peroxymonosulfate, Chem Eng J 356 (2019) 1022–1031.
[34] M.-H. Li, K.-Y.A. Lin, M.-T. Yang, B.X. Thanh, D.C.W. Tsang, Prussian Blue Analogue-derived co/fe bimetallic nanoparticles immobilized on S/N-doped carbon sheet as a magnetic heterogeneous catalyst for activating peroxymonosulfate in water, Chemosphere 244 (2020), 125444.
[35] Q. Xiao, S. Yu, Reduction of bromate from drinking water by sulfite/ferric ion systems: Efficacy and mechanisms, J Hazard Mater 418 (2021), 125940.
[36] Y. You, H. Yuan, Y. Wu, Y. Ma, C. Meng, X. Zhao, A novel red phosphorus/perylene diimide metal-free photocatalyst with p-n heterojunctions for efficient photoreduction of bromate under visible light, Sep Purif Technol 264 (2021), 118456.
[37] D. Zhao, J. Dai, N. Zhou, N. Wang, P. Xinwen, Y. Qu, L. Li, Prussian blue analogues-derived carbon composite with cobalt nanoparticles as an efficient bifunctional electrocatalyst for oxygen reduction and hydrogen evolution, Carbon 142 (2019) 196–205.
[38] X. Zeng, B. Yang, L. Zhu, H. Yang, R. Yu, Structure evolution of Prussian blue analogues to CoFe@C core–shell nanocomposites with good microwave absorbing performances, RSC Adv 6 (2016) 105644–105652.
[39] M. Hu, S. Ishihara, K. Ariga, M. Imura, Y. Yamauchi, Kinetically Controlled Crystallization for Synthesis of Monodispersed Coordination Polymer Nanocubes and Their Self-Assembly to Periodic Arrangements, Eur. J. Chem. 19 (2013) 1882–1885.
[40] W. Mei, J. Huang, L. Zhu, Z. Ye, Y. Mai, J. Tu, Synthesis of porous rhombus-shaped Co3O4 nanorod arrays grown directly on a nickel substrate with high electrochemical performance, J Mater Chem 22 (2012) 9315–9321.
[41] J. Zhang, Z. Lyu, F. Zhang, L. Wang, P. Xiao, K. Yuan, M. Lai, W. Chen, Facile synthesis of hierarchical porous Co3O4 nanoboxes as efficient cathode catalysts for Li-O2 batteries, J. Mater. Chem. A 4 (2016) 6350–6356.
[42] C.-W. Tang, C.-B. Wang, S.-H. Chien, Characterization of cobalt oxides studied by FT-IR, Raman, TPR and TG-MS, Thermochimica Acta 473 (2008) 68–73.
[43] S. Zhao, F. Hu, J. Li, Hierarchical Core-Shell Al2O3@Pd-CoAlO Microspheres for Low-Temperature Toluene Combustion, ACS Catal 6 (2016) 3433–3441.
[44] Q. Liu, L.-C. Wang, M. Chen, Y. Cao, H.-Y. He, K.-N. Fan, Dry citrate-precursor synthesized nanocrystalline cobalt oxide as highly active catalyst for total oxidation of propane, J Catal 263 (2009) 104–113.
[45] X. Wang, Y. Liu, T. Zhang, Y. Luo, Z. Lan, K. Zhang, J. Zuo, L. Jiang, R. Wang, Geometrical-Site-Dependent Catalytic Activity of Ordered Mesoporous Co-Based Spinel for Benzene Oxidation, Situ DRIFTS Study Coupled with Raman and XAFS Spectroscopy, ACS Catalysis 7 (2017) 1626–1636.
[46] Z. Yang, M. Xu, Y. Liu, F. He, F. Gao, Y. Su, H. Wei, Y. Zhang, Nitrogen-doped, carbon-rich, highly photoluminescent carbon dots from ammonium citrate, Nanoscale 6 (2014) 1890–1895.
[47] N. Dwivedi, R.J. Yeo, N. Satyanarayana, S. Kundu, S. Tripathy, C.S. Bhatia, Understanding the Role of Nitrogen in Plasma-Assisted Surface Modification of Magnetic Recording Media with and without Ultrathin Carbon Overcoats, Sci Rep 5 (2015) 7772.
[48] M. Kang, M.W. Song, C.H. Lee, Catalytic carbon monoxide oxidation over CoOx/CeO2 composite catalysts, Appl Catal A 251 (2003) 143–156.
[49] J. Li, G. Lu, G. Wu, D. Mao, Y. Guo, Y. Wang, Y. Guo, Effect of TiO2 crystal structure on the catalytic performance of Co3O4/TiO2 catalyst for low-temperature CO oxidation, Catal Sci Technol 4 (2014) 1268–1275.
[50] Y. Chen, Q. Wang, C. Zhu, P. Gao, Q. Ouyang, T. Wang, Y. Ma, C. Sun, Graphene/porous cobalt nanocomposite and its noticeable electrochemical hydrogen storage ability at room temperature, J Mater Chem 22 (2012) 5924–5927.
[51] Y. Yao, C. Xu, J. Qin, F. Wei, M. Rao, S. Wang, Synthesis of Magnetic Cobalt Nanoparticles Anchored on Graphene Nanosheets and Catalytic Decomposition of Orange II, Ind Eng Chem Res 52 (2013) 17341–17350.
[52] Z. Xu, J. Lu, Q. Liu, L. Duan, A. Xu, Q. Wang, Y. Li, Decolorization of Acid Orange II dye by peroxymonosulfate activated with magnetic Fe3O4@C/Co nanocomposites, RSC Adv 5 (2015) 76862–76874.
[53] J. Liu, T. Zhang, Z. Wang, G. Dawson, W. Chen, Simple pyrolysis of urea into graphitic carbon nitride with recyclable adsorption and photocatalytic activity, J Mater Chem 21 (2011) 14398–14401.
[54] C. Wu, F. Wu, Y. Bai, B.L. Yi, H.M. Zhang, Cobalt boride catalysts for hydrogen generation from alkaline NaBH4 solution, Mater Lett 59 (2005) 1748–1751.
[55] R. Krishna, D.M. Fernandes, C. Dias, J. Ventura, E. Venkata Ramana, C. Freire, E. Titus, Novel synthesis of Ag@Co/RGO nanocomposite and its high catalytic activity towards hydrogenation of 4-nitrophenol to 4-aminophenol, Int J Hydrogen Energy 40 (2015) 4996–5005.
[56] J. Restivo, O.S.G.P. Soares, J.J.M. Órfão, M.F.R. Pereira, Metal assessment for the catalytic reduction of bromate in water under hydrogen, Chem Eng J 263 (2015) 119–126.
[57] T. Wi-Afedzi, E. Kwon, D.D. Tuan, K.-Y.A. Lin, F. Ghanbari, Copper hexacyanoferrate nanocrystal as a highly efficient non-noble metal catalyst for reduction of 4-nitrophenol in water, Sci Total Environ 703 (2020), 134781.
[58] D.D. Tuan, K.-Y.A. Lin, Ruthenium supported on ZIF-67 as an enhanced catalyst for hydrogen generation from hydrolysis of sodium borohydride, Chem Eng J 351 (2018) 48–55.
[59] T. Wi-Afedzi, F.-Y. Yeoh, M.-T. Yang, A.C.K. Yip, K.-Y.A. Lin, A comparative study of hexacyanoferrate-based Prussian blue analogue nanocrystals for catalytic reduction of 4-nitrophenol to 4-aminophenol, Sep Purif Technol 218 (2019) 138–145.
[60] K.-Y.A. Lin, C.-H. Lin, Simultaneous reductive and adsorptive removal of bromate from water using acid-washed zero-valent aluminum (ZVAl), Chem Eng J 297 (2016) 19–25.
[61] K.-Y.A. Lin, C.-H. Lin, H. Yang, Enhanced bromate reduction using zero-valent aluminum mediated by oxalic acid, J Environ Chem Eng 5 (2017) 5085–5090.
[62] C.-H. Liu, B.-H. Chen, C.-L. Hsueh, J.-R. Ku, M.-S. Jeng, F. Tsau, Hydrogen generation from hydrolysis of sodium borohydride using Ni–Ru nanocomposite as catalysts, Int J Hydrogen Energy 34 (2009) 2153–2163.
[63] L. Ai, X. Liu, J. Jiang, Synthesis of loofah sponge carbon supported bimetallic silver–cobalt nanoparticles with enhanced catalytic activity towards hydrogen generation from sodium borohydride hydrolysis, J Alloy Compd 625 (2015) 164–170.
[64] S.G.S. Santos, L.O. Paulista, T.F.C.V. Silva, M.M. Dias, J.C.B. Lopes, R.A. R. Boaventura, V.J.P. Vilar, Intensifying heterogeneous TiO2 photocatalysis for bromate reduction using the NETmix photoreactor, Sci Total Environ 664 (2019) 805–816.
[65] X. Zhao, Y. You, S. Huang, F. Cheng, P. Chen, H. Li, Y. Zhang, Facile construction of reduced graphene oxide supported three-dimensional polyaniline/WO2.72

nanobelt-flower as a full solar spectrum light response catalyst for efficient photocatalytic conversion of bromate, Chemosphere 222 (2019) 781–788.
[66] S. Nawaz, N.S. Shah, J.A. Khan, M. Sayed, A.a.H. Al-Muhtaseb, H.R. Andersen, N. Muhammad, B. Murtaza, H.M. Khan, Removal efficiency and economic cost comparison of hydrated electron-mediated reductive pathways for treatment of bromate, Chem Eng J 320 (2017) 523–531.
[67] K.-Y. Andrew Lin, S.-Y. Chen, Bromate reduction in water by catalytic hydrogenation using metal–organic frameworks and sodium borohydride, RSC, Advances 5 (2015) 43885–43896.